

# Distribution-Informed Adaptation for kNN Graph Construction

Min Shaojie  
Chongqing University  
Chongqing, China  
alexmin@cqu.edu.cn

Liu Ji  
Chongqing University  
Chongqing, China  
liujiboy@cqu.edu.cn

## ABSTRACT

Graph-based kNN algorithms have garnered widespread popularity for machine learning tasks due to their simplicity and effectiveness. However, as factual data often inherit complex distributions, the conventional kNN graph’s reliance on a unified  $k$ -value can hinder its performance. A crucial factor behind this challenge is the presence of ambiguous samples along decision boundaries that are inevitably more prone to incorrect classifications. To address the situation, we propose the **Distribution-Informed adaptive kNN Graph (DaNNG)**, which combines adaptive kNN with distribution-aware graph construction. By incorporating an approximation of the distribution with customized  $k$ -adaption criteria, DaNNG can significantly improve performance on ambiguous samples, and hence enhance overall accuracy and generalization capability. Through rigorous evaluations on diverse benchmark datasets, DaNNG outperforms state-of-the-art algorithms, showcasing its adaptability and efficacy across various real-world scenarios.

## CCS CONCEPTS

• **Networks** → **Topology analysis and generation**; • **Computing methodologies** → **Machine learning approaches**; *Supervised learning by classification.*

## KEYWORDS

Graph-Based Algorithm, Machine Learning, Adaptive kNN Graph

## 1 INTRODUCTION

In the realm of data science and machine learning, the  $k$ -Nearest Neighbors (kNN) algorithm has emerged as a fundamental yet powerful tool for a wide range of classification and regression tasks. Its simplicity, single-parametric nature, and ability to capture local patterns make it a popular choice in various domains, including image recognition [12], natural language processing [30], and recommendation systems [1]. Despite its popularity and ease of implementation, the traditional kNN approach comes with inherent limitations that can affect its performance and applicability in certain scenarios.

One of the primary limitations of traditional kNN lies in its dependence on feature-based representations, potentially disregarding deep-level relationships and dependencies among data points. To address this limitation, researchers have explored the use of kNN graph (kNNG) [4, 6, 8], where each data point is connected to its  $k$  nearest neighbors in the feature space. As a graph-based approach, kNNG opened the avenue for capturing data relationships via graph-theory methodologies that can uncover the inherent data connections more effectively.

However, in kNNG, the inherited unified- $k$  across all data points can still result in compromised generalization capabilities, especially in scenarios where the underlying data distribution exhibits complex patterns. Researchers have shown that adaptively determining  $k$  values can improve the algorithm’s robustness. Adaptive methods for kNNG, as well as kNN, often adjust  $k$ -value under the guidance of certain criteria, such as regional accuracy [9] or local density [5]. Local distribution information has also been introduced into the determination process, such as the adaKNN [27], SMKNN [3], and DC-LAKNN [22], aiming to enhance the performance with the aid of the varying local density.

A critical challenge for cutting-edge adaptive kNNG algorithms stems from ambiguous samples. The ambiguous samples can be defined as:

*Definition 1.1 (Ambiguous Samples).* Ambiguous samples<sup>1</sup>, or borderline samples, refer to samples that lie close to the decision boundaries among different classes.

Ambiguous samples’ approximation to other classes makes them difficult to be predicted [20, 24]. Improving performance on borderline samples will naturally lead to a more satisfactory overall performance.

In this paper, we demonstrate that integrating an approximation of the original data distribution as a cohesive entity is naturally suitable to adaptively determine  $k$  and solve the predicament posed by borderline samples. We present a novel approach called the **Distribution-Informed adaptive kNN Graph (DaNNG)** which incorporates distribution’s approximation into the construction of a heterogeneous graph representation. The distribution-informed DaNNG learns an approximation of overall distribution, within which the  $k$  values for borderline samples are adapted under guidance of customized criteria. It then leverages the acquired distribution-based information and traditional  $k$ -value to reach an optimal  $k$ -sequence for data. Under rigorous evaluations, we achieve significant performance gain on borderline samples, resulting in improved overall accuracy and generalization capability.

## 2 RELATED WORK

The concept of adaptive- $k$  in kNN algorithms focuses on dynamically determining the optimal value of  $k$  for each data point, while graph-based kNN methods leverage graph structures to represent and analyze data relationships. Both adaptive kNN and graph-based kNN methods have shown promising results in improving the performance of traditional kNN.

<sup>1</sup>Ambiguous samples will be refer to as “borderline samples” to highlight their characteristic.

## 2.1 Adaptive kNN

Adaptive kNN algorithms offer the advantage of dynamically determining the optimal k-value for each data point, allowing the model to adapt to varying data densities and achieve improved performance in complex and diverse datasets. One notable development in the area of adaptive kNN is the work of Ada-kNN2 by Mullick et al. [17]. The author addressed the challenge of varying densities across data regions by learning suitable k-value from the test-point neighborhood with the help of artificial neural networks. Similarly, Jodas et al. presented the parameterless nearest neighbors classifier (PL-kNN) [15], where  $k$  is automatically adjusted based on the underlying data characteristics, alleviating the need for manual parameter tuning. A tree-based adaptive kNN, named KTree, was developed by Zhang et al. [34], in which optimal-k can be efficiently obtained for test samples from a pre-constructed decision tree. The proposed KTree exhibits improved resilience to class imbalance, enhancing the robustness of kNN classifiers in challenging data scenarios.

## 2.2 Graph-Based kNN

Graph-based kNN approaches (i.e., kNNG) leverage graph structures to represent data relationships, enabling a more intuitive and interpretable representation of data. One example is the concept of the centered kNNG introduced by Suzuki and Hara [28] for semi-supervised learning. Centered kNNG aims to reduce the presence of hubs by eliminating common directions of inner-product on the Hilbert space, which not only enhances robustness but also incurs minimal computational overhead.

Like adaptive kNN, kNN Graph can also adopt adaptive strategies to determine  $k$  values, resulting in graphs exhibiting heterogeneity in node degrees. The AKNNG [5] dynamically adjusts the number of neighbors with an enhanced similarity matrix to explore optimal-k and its application in spectral clustering. Murrugarra-Llerena and Andrade Lopes [18] presented an adaptive graph-based kNN method that iteratively adjusts neighbor numbers for misclassified samples. Furthermore, Yan et al. [33] introduced a robust gravitation-based approach addressing the challenges of class-imbalanced scenarios in kNNG.

Distribution's significance in the determination of  $k$  for kNNG has been verified in previous works, including [18, 33, 34]. These methods have demonstrated the advantages of considering data distribution as model inputs, leading to more accurate and robust representations of data relationships. However, existing approaches neglect the interrelation between borderline samples and data distribution, potentially limiting their ability to capture underlying relationships within the data. In contrast, our DaNNG integrates the data distribution while simultaneously considering the behaviour of borderline samples'  $k$ , substantially improving borderline-sample accuracy, and hence strengthening overall model robustness.

## 3 PRELIMINARIES

### 3.1 The k-Nearest Neighbors Graph (kNNG)

The kNNG can be considered as a representation of kNN but with more flexible graph-based prediction strategies. For  $n \times d$  data  $X$  and a given  $n \times n$  similarity matrix  $S$ , we generate a  $n \times n$  binary matrix  $W$

such that  $W_{ij} = 1$  iff.  $j \in NN_k(X_i)$ . A plain kNNG is an undirected graph  $G = (V, E)$  in which  $V_i$  represents the  $i_{th}$  sample in  $X$  and the corresponding adjacent matrix  $A$  is determined as  $A_{ij} = A_{ji} = 1$  iff.  $(W_{ij} = 1) \vee (W_{ji} = 1)$ . For more complicated situations, a mutual kNNG indicates  $A_{ij}^{mutual} = A_{ji}^{mutual} = 1$  iff.  $(W_{ij} = 1) \wedge (W_{ji} = 1)$ , whereas a directed kNNG has  $A_{ij}^{directed} = 1$  iff.  $W_{ij} = 1$ .

### 3.2 The Kullback-Leibler Divergence

The Kullback-Leibler (KL) Divergence, also known as relative entropy, is a fundamental concept in information theory and statistics. Introduced by Solomon Kullback and Richard Leibler in the 1950s, KL divergence measures the dissimilarity between two probability distributions. The original KL divergence formula is given by:

$$D_{KL}(P||Q) = \sum_i p_i \log \frac{p_i}{q_i} \quad (1)$$

where  $P$  and  $Q$  are two probability distributions.

In our model, The concept of KL divergence is exploited to measure the sample-wise estimation rather than the value-oriented distribution, aiming to acquire the fitness kernel  $F$ .

### 3.3 The Fitness Kernel

The fitness kernel, originally referred to as a mathematical function that quantifies the fitness or suitability of nodes in a network under the context of network science, is utilized to determine  $k$  for each sample in our model.

Given a set of  $d$ -dimensional vectors  $X = \{x_1, x_2, \dots, x_n\} \in \mathbb{R}^{n \times d}$ , we define the fitness kernel  $F = \{f_1, f_2, \dots, f_n\} \in \mathbb{R}^{n \times 1}$  as a one-dimensional vector, serving as an approximation of the data distribution with suitable variation.

### 3.4 Research Objective

Given a  $d$ -dimensional vector  $X \in \mathbb{R}^{n \times d}$ , our objective is to construct an adaptive kNNG,  $G = (V, E)$ , called the Distribution-Informed adaptive kNN Graph (DaNNG), aiming to effectively improve performance on borderline samples and thus enhance overall robustness.

### 3.5 Quantified Borderline Samples

To facilitate quantitative evaluation, borderline samples are quantified as follows:

*Definition 3.1 (i-Quantile Borderline).* The  $i$ -Quantile Borderline, denoted as  $iQB$ , refers to a subset of samples whose probability estimations lie in the lower  $i$  percent of the population.

### 3.6 Distribution-Informed Adaption

In this section, we demonstrate why introducing overall distribution to the adaption of  $k$  can be rewarding.

Assuming the subsamples within a classification task are several Gaussian-distributed clusters, a unified  $k$  for samples on the cluster border will inevitably include samples from other classes, bringing uncertainty into prediction. To elaborate, we provide an intuitive illustration via two-class (blue and red) data  $X = \{x_1, x_2, \dots, x_{17}\}$  in Figure 1.

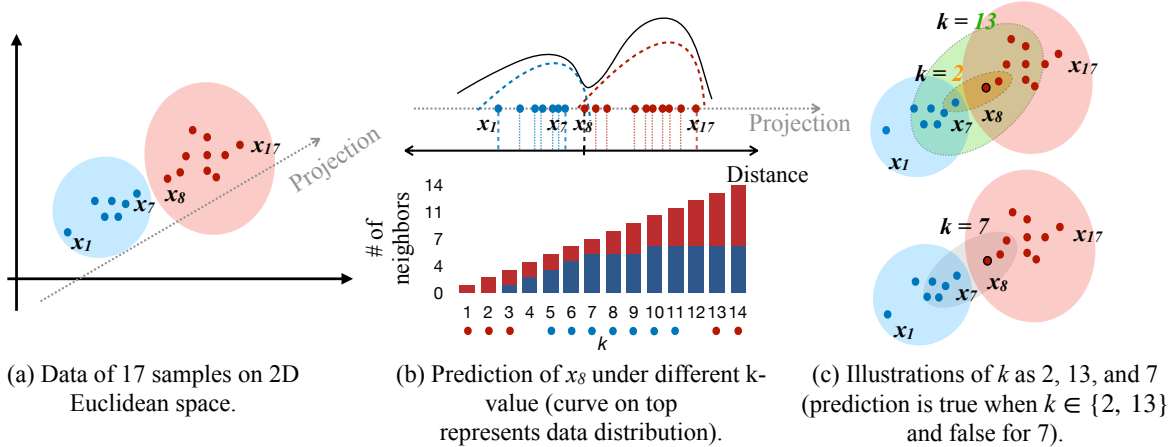


**Figure 1: Demonstration of borderline-sample misclassification under data containing two left-skewed classes.**

Under the projection direction,  $x_1, x_7$  and  $x_8, x_{17}$  are at the border of each class (i.e., borderline samples). If we try different values of  $k$  to classify the borderline sample  $x_8$ , we will observe a false prediction (blue) under common  $k$  values (from 5 to 11). This pattern is strengthened if different classes exhibit the same side of skewness (two classes in Figure 1(b) are both left-skewed).

A viable solution is to assign larger/smaller  $k$  for borderline samples, aiming to achieve the following:

- Smaller- $k$ : This choice favors a narrower range of samples, prioritizing the closest neighbors that are more likely to belong to the same class.
- Larger- $k$ : Including a larger range of samples in the process helps to capture more comprehensive information.

In the provided example, it becomes evident that both opting for smaller- $k$  and choosing larger- $k$  can lead to accurate results. (predicted 'red' when  $k \in \{1, 2, 3\}$  or  $k \in \{13, 14\}$ ).

This pattern of the  $k$ -value, evolving  $k$  to either larger or smaller for borderline samples, is reconciled with the distribution of data because no matter whether  $k$  becomes larger or smaller the corresponding probability estimation will both become lower. In other words, patterns of low probability estimation for borderline samples align with the low probability estimations for their  $k$  values after adaption, making the overall distribution information an ideal choice of input for  $k$ -determination.

## 4 METHODOLOGY

The Distribution-Informed adaptive kNN Graph (DaNNG) model is presented in this section. The construction of DaNNG can be summarized as the adaptive determination of the value of  $k$  for each data point with the pre-learned fitness kernel,  $F$ , which approximates the original distribution under the guidance of local topology on borderline samples.

### 4.1 Determining $k$

The  $k$  values for samples in DaNNG are determined using the following formula:

$$K = (1 - \eta)\kappa + \eta F + \epsilon \quad (2)$$

where  $K \in \mathbb{R}^{n \times 1}$  represents the corresponding  $k$  value for each sample,  $\eta \in [0, 1]$  is the parameter controlling the trade-off between traditional  $k$  (i.e.,  $\kappa$ ) and the fitness kernel  $F$ . Additionally,  $\epsilon \in \mathbb{R}^{n \times 1}$  is a random vector in which  $\epsilon_i \sim \mathcal{N}(0, \frac{1}{3})$  accounting for stochastic variations that can only increase/decrease  $k_i$  by 1 at most ( $3\sigma = 1$ ).

### 4.2 Acquiring the Fitness Kernel

We aim to acquire a fitness kernel,  $F$ , that approximates the original distribution. In DaNNG,  $F$  is obtained through a two-step process wherein the objective is to iteratively minimize sample-wise Kullback-Leibler divergence under customized constraints.

**4.2.1 Initialization of  $F$ .** We initialize the fitness kernel  $F$  by assigning equal values to each data point in the same classes, in which higher values are assigned to dense regions to achieve high level of clustering. This serves as the starting point for the iterative process of minimizing the KL divergence.

Given a dataset with  $m$  classes of samples:

$$X = \{x_1, x_2, \dots, x_n\} \in \mathbb{R}^{n \times d}, y = \{y_1, y_2, \dots, y_n \in C\} \in \mathbb{R}^{n \times 1} \quad (3)$$

where  $C = \{c_1, c_2, \dots, c_m\}$  represents target labels.

We initialize  $F$  as:

$$F_{\text{init}} = \log N_{y_i} \quad (4)$$

where  $N_{y_i}$  is the sample count of class  $y_i$ , and the logarithm aims to prevent a cascade effect in which classes with large amounts of samples may result in a fully connected graph.

**Algorithm 1** Acquire Fitness Kernel

**Input:**  $X, y$  - Data matrix of size  $(n, d)$  and prediction target of size  $(n, 1)$

**Output:**  $F$  - Vector of fitness kernel in  $(n, 1)$

- 1: Initialize  $F$  with Equation 4:  $F_{\text{init}} = \log(\text{bincount}(y))$
- 2: Let  $F = F_{\text{init}}$  and  $\text{loss} = 1$
- 3: Compute sample-wise  $X_{\text{probs}}$
- 4: Set  $\text{threshold} = 1e - 2$
- 5: **while**  $\text{loss} > \text{threshold}$  **do**
- 6:   Compute sample-wise  $F_{\text{probs}}$
- 7:   Compute  $\text{loss}$  with Equation 7:  
 $\text{loss} = \text{KLDivergence}(X_{\text{probs}}, F_{\text{probs}})$  s.t.  $g(F) \leq 0$
- 8:   **if**  $\text{loss} < \text{threshold}$  **then**
- 9:     **break**
- 10:   **end if**
- 11:   Update  $F$ :  $F = F - \text{learning\_rate} \times \text{loss}$
- 12: **end while**
- 13: Normalize  $F$ :  $F_{\text{scaled}} = \text{Scale}(F, \min = \frac{1}{2}\kappa, \max = \frac{3}{2}\kappa)$
- 14: **return**  $F_{\text{scaled}}$

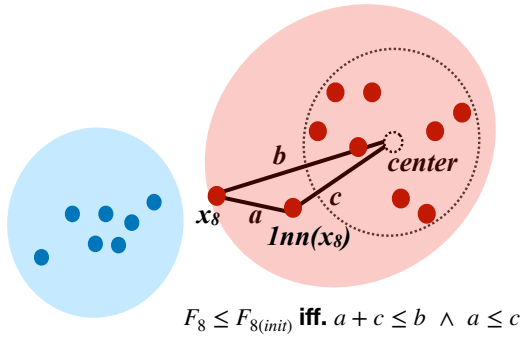


**Figure 2: Criteria demonstration of circumstance when  $F$  evolves to smaller value for borderline samples.**

**4.2.2 Adaption Criteria for Borderline Samples.** As elucidated in Section 3.6, borderline samples exhibit two directions of evolution, one towards larger values of  $k$  and the other towards smaller  $k$ , both of which can potential enhance model robustness. To discern which direction is the most appropriate for each sample in the process of optimizing KL Divergence, we devised a straightforward rule based on the strong correlation between the proximity of the nearest neighbor (1NN) and smaller  $k$  (as elaborated in Section 3.6).

This rule is derived from the local topology and prescribes the adoption of a smaller  $k$  exclusively for borderline sample that meet the following conditions:

- The shortest path to the center of its class (excluding the sample itself and its nearest neighbor) traverses through the nearest neighbor (i.e.,  $a + c \leq b$  in Figure 2).
- The distance to their nearest neighbor is either equal to or less than the distance between the nearest neighbor and the class center (i.e.,  $a \leq c$  in Figure 2).

In Figure 2, we have demonstrated the determination criteria of the smaller- $k$  evolution for  $x_8$ . This criteria for borderline samples can be formally represented as constraints during distribution approximation in the form:

$$g(F) \leq 0, \text{ s.t. } g_i(F) = \begin{cases} f_i - f_i^{\text{init}}, & i \in S \\ f_i^{\text{init}} - f_i, & i \in H \end{cases} \quad (5)$$

in which  $S$  and  $H$  are two subsets of the borderline set (i.e.,  $S, H \subseteq iQB$ ) that meet:

$$\begin{cases} x_i \in S \text{ iff. } \text{dist}(x_i, 1\text{NN}(x_i)) < \text{dist}(1\text{NN}(x_i), \mu_i) \\ \quad \wedge \text{dist}(x_i, 1\text{NN}(x_i)) + \text{dist}(1\text{NN}(x_i), \mu_i) \leq \text{dist}(x_i, \mu_i), \\ H = iQB - S \end{cases} \quad (6)$$

where  $\mu_i$  is the class center of  $y_i$  excluding  $x_i$  and  $1\text{NN}(x_i)$ .

To assess the effectiveness of our proposed criteria, we have added a version of DaNNG during evaluations in Section 6.

**4.2.3 Approximate Original Distribution.** Since the KL divergence is originally intended for measuring similarities between two populations and is not suitable for comparing  $d$ -dimensional  $X$  and one-dimensional  $F$ , we design a loss by modifying KL divergence to measure the dissimilarity of sample-wise probability between  $X$  and  $F$  instead:

$$\text{loss} = \sum_{i=1}^n P(x_i) \cdot \log\left(\frac{P(x_i)}{P(f_i)}\right), \text{ s.t. } g(F) \leq 0 \quad (7)$$

where  $P(x_i)$  and  $P(f_i)$  are the probabilities for the  $i$ -th sample in  $X$  and  $F$ , respectively.

The loss function is used to modify  $F$  so that the fitness kernel preserves the original data distribution while the fitness values for borderline samples evolve to the intended directions under the guidance of constraint,  $g(F) \leq 0$ . In DaNNG, we calculate the probability via Kernel Density Estimation (KDE), yielding the slope of gradient descent becomes:

$$\begin{aligned} \nabla = \frac{\partial \text{loss}}{\partial F} = & \frac{1}{h^2 \rho} \left( \rho \sum_{i=1}^n P(x_i)(F - f_i) \right. \\ & \left. + P(X) \sum_{i=1}^n \rho_i(F - f_i) \right) \quad (8) \end{aligned}$$

where  $\rho$  represents the KDE under Gaussian kernel, i.e.,  $\rho_i = \sum_{j=1}^n e^{-\frac{1}{2h^2}(f_i - f_j)^2}$  and  $h$  is the bandwidth controlling distribution smoothing. Additionally, to ensure a consistent impact across different  $\kappa$ ,  $F$  is scaled proportionally to range  $(\frac{1}{2}\kappa, \frac{3}{2}\kappa)$  (Proof and analysis provided in Section 5).

### 4.3 Graph Construction

With  $K$  determined and a given similarity measurement, the binary matrix  $W$  for DaNNG is obtained as:

$$W_{ij}^{\text{DaNNG}} = \begin{cases} 1, & \text{if } j \in k\text{NN}_{k_i}(x_i) \\ 0, & \text{if } j \notin k\text{NN}_{k_i}(x_i) \end{cases} \quad (9)$$

Using the same construction procedures described in Section 3, the adjacent matrix  $A$  for DaNNG is obtained as  $A_{\text{DaNNG}} = \max(W_{\text{DaNNG}}, W_{\text{DaNNG}}^T)$ ,  $A_{\text{DaNNG}}^{\text{directed}} = W_{\text{DaNNG}}$  for direct DaNNG, and  $A_{\text{DaNNG}}^{\text{mutual}} = \min(W_{\text{DaNNG}}, W_{\text{DaNNG}}^T)$  for mutual DaNNG.

---

**Algorithm 2** DaNNG Construction
 

---

**Input:**  $X$ ,  $y$ , and  $k$  - Data matrix of size  $(n, d)$ , prediction target of size  $(n, 1)$  and user-defined  $k$  of traditional kNN Graph

**Output:**  $A$  - Adjacency matrix  $(n, n)$  of DaNNG

- 1: Compute  $F$  using Algorithm 1
  - 2: Compute  $\eta_m = \arg \max_{\eta} (\text{Accuracy})$  **for**  $\eta \in (0, 1)$
  - 3: Let  $K = (1 - \eta_m) \cdot \kappa + \eta_m \cdot F + \epsilon \sim \mathcal{N}(0, \sigma^2)$
  - 4: Set  $W_{\text{DaNNG}} = \text{zeros}(n, n)$
  - 5: **for** each sample  $i$  **do**
  - 6:   Compute  $kNN_i = k_i \text{NearestNeighbors}(i)$
  - 7:   **for**  $j$  in  $kNN_i$  **do**
  - 8:     Set the corresponding entries in  $W_{\text{DaNNG}}$  to 1:  $W_{\text{DaNNG}}^{(i,j)} = 1$
  - 9:   **end for**
  - 10: **end for**
  - 11:  $A_{\text{DaNNG}} = \max(W_{\text{DaNNG}}, W_{\text{DaNNG}}^T)$
  - 12: **return**  $A_{\text{DaNNG}}$
- 

After the graph is constructed, various graph-based algorithms, such as label propagation [16], can be employed to make predictions.

## 5 THEORETICAL ANALYSIS

In this section, we first provide how we solve the constrained optimization in practice, and then establish that the scaling of  $F$  is dispensable in DaNNG as long as it upholds symmetry in relation to  $\kappa$ .

### 5.1 Constrained Optimization for KL Divergence

With the pre-defined sample-wise KL divergence loss in Formula 7, we illustrate how we obtain the slope of the gradient loss in Equation 8.

Since  $P(X)$  is fixed, the optimization objective can be reformulated as:

$$\min_{F \in \mathbb{R}^{n \times 1}} \sum_{i=1}^n P(x_i) \cdot \log \left( \frac{P(x_i)}{P(f_i)} \right), \text{ s.t. } g(F) \leq 0 \quad (10)$$

**5.1.1 Gradient of Loss.** In practice, with Gaussian kernel KDE as the probability measurement, we have:

$$\begin{aligned} \frac{\partial \text{loss}}{\partial F} &= -\sum_{i=1}^n P(x_i) \log \sum_{j=1}^n K(f_i - f_j, h) \\ &= -\sum_{i=1}^n P(x_i) \log \sum_{j=1}^n e^{-\frac{1}{2h^2}(f_i - f_j)^2} \end{aligned} \quad (11)$$

where  $K(\cdot)$  and  $h$  are the kernel and bandwidth of KDE, respectively. For each projection of  $F$ , we have:

$$\begin{aligned} \frac{\partial \text{loss}}{\partial f_m} &= \frac{1}{h^2} \left( \sum_{i=1}^n P(x_i) (f_m - f_i) \right. \\ &\quad \left. + P(x_m) \frac{\sum_{i=1}^n (f_m - f_i) e^{-\frac{1}{2h^2}(f_m - f_i)^2}}{\sum_{i=1}^n e^{-\frac{1}{2h^2}(f_m - f_i)^2}} \right) \\ &= \frac{1}{h^2 \rho_m} \left( \rho_m \sum_{i=1}^n P(x_i) (f_m - f_i) \right. \\ &\quad \left. + P(x_m) \sum_{i=1}^n \rho_{m,i} (f_m - f_i) \right) \end{aligned} \quad (12)$$

where  $\rho_m$  is the estimation of  $f_m$ , i.e.,  $\rho_m = \sum_{i=1}^n e^{-\frac{1}{2h^2}(f_m - f_i)^2}$ .

**5.1.2 Optimization under Inequality Constraints.** The constrained optimization is handled by the method of Lagrange multipliers with the Karush-Kuhn-Tucker (KKT) conditions.

The Lagrangian  $L(F, \lambda)$  for our problem is given by:

$$L(F, \lambda) = \text{loss} + \lambda g(F) \quad (13)$$

where  $\lambda$  is the Lagrange multiplier associated with the inequality constraint.

The associated KKT conditions are as follows:

$$\begin{aligned} \nabla_F L(F, \lambda) &= \frac{\partial \text{loss}}{\partial F} + \lambda \nabla g(F) = 0 \\ \text{s.t. } g(F) &\leq 0, \lambda \geq 0, \lambda g(F) = 0 \end{aligned} \quad (14)$$

With the slope of gradient clarified in the previous section, we can perform gradient descent using a properly chosen optimization algorithm, such as Sequential Least Squares Quadratic Programming (SLSQP).

### 5.2 Normalization Equivalence

Theoretically speaking, our approach will not guarantee the obtained  $F$  falling into a specific range. Practical reasoning concludes that  $F$  should be appropriately scaled in order not to jeopardize the impact of  $\kappa$  in Formula 2.

In this section, we prove that the scaling of  $F$  is not necessary in DaNNG as long as it maintains symmetric about  $\kappa$ .

**PROOF.** A formal restatement of this matter can be summarized as follows:

$$\begin{aligned} \forall F_1 &= g_1(F), F_2 = g_2(F), \kappa \in \mathbb{R} \\ \exists \eta_1, \eta_2, \text{ s.t. } &(1 - \eta_1)\kappa + \eta_1 F_1 \\ &\equiv (1 - \eta_2)\kappa + \eta_2 F_2 \end{aligned} \quad (15)$$

where  $g(\cdot)$  denotes the normalization of mapping  $F$  into range  $(\text{Min}, \text{Max})$ ,  $g(F) = \frac{(F - f_{\text{min}}) \times (\text{Max} - \text{Min})}{f_{\text{max}} - f_{\text{min}}} + \text{Min}$ , s.t.  $(\text{Max}_i \neq \text{Min}_i) \wedge (\frac{\text{Max}_i + \text{Min}_i}{2} = \kappa)$ .

**THEOREM 5.1.** *Bijjective Linear Transformation – the normalization of  $g(\cdot) : \mathbb{R}^{n \times 1} \rightarrow \mathbb{R}^{n \times 1}$  indicates a self-explanatory bijjective linear transformation between vector spaces that are both injective (one-to-one) and surjective (onto), implying that it has a unique inverse iff.  $\text{Max} \neq \text{Min}$ .*

Because of Theorem 5.1, the identity in formula 15 becomes:

$$\eta_1 g_1(g_2^{-1}(F_2)) - \eta_2 F_2 + (\eta_2 - \eta_1) \kappa \equiv 0 \quad (16)$$

With  $g(F) = \frac{(F-f_{min}) \times (Max-Min)}{f_{max}-f_{min}} + Min$  and  $F_2 \in \mathbb{R}^{n \times 1}$ , we have:

$$\begin{cases} \frac{Max_1 - Min_1}{Max_2 - Min_2} \times \eta_1 - \eta_2 = 0 \\ (Min_1 - \kappa)\eta_1 + (\kappa - Min_2)\eta_2 = 0 \end{cases} \quad (17)$$

where  $Max_i$  and  $Min_i$  represent the target range of the  $i_{th}$  normalization.

To determine whether the above homogeneous system have solutions for  $\eta_1$  and  $\eta_2$ , we rewrite the corresponding coefficient matrix:

$$\begin{bmatrix} 1 & -\frac{1}{\alpha} \\ 0 & \alpha(\kappa - Min_2) - (\kappa - Min_1) \end{bmatrix} \quad (18)$$

in which  $\alpha$  represents the fraction of ranges (i.e.,  $\alpha = \frac{Max_1 - Min_1}{Max_2 - Min_2}$ ). The coefficient matrix has rank 1 iff.  $(Max_i \neq Min_i) \wedge (\frac{Max_i + Min_i}{2} = \kappa)$ .  $\square$

Thus, there exist solutions as  $\eta_2 = \alpha \times \eta_1$ , s.t.  $(\alpha = \frac{Max_1 - Min_1}{Max_2 - Min_2}) \wedge (Max_i \neq Min_i)$  for any pair of  $\kappa$ -symmetric normalizations  $g_1(\cdot)$  and  $g_2(\cdot)$  to be equivalent. In other words, although we scale  $F$  to  $(\frac{1}{2}\kappa, \frac{3}{2}\kappa)$  to ensure consistent impacts across different  $\kappa$ , the flexibility of the model is enriched by automatically incorporating various ranges through the trade-off parameter  $\eta$  without requiring any additional procedures.

## 6 EVALUATIONS

### 6.1 Experiment Settings

Dataset	Instances	Classes	Dimensions
WDBC	569	2	30
BCC	116	2	9
WPBC	198	2	30
Heart Disease	303	4	13
Abalone	4177	28	8
Glass	214	6	9
Zoo	101	7	16
Glioma	839	2	23
Diabetes	768	2	7
Dermatology	366	6	34
Wine	178	3	13
German Credit	1000	2	20

Table 1: Statistics of included datasets.

We evaluate DaNNG’s performance on both binary classification and multi-class classification tasks against nine state-of-the-art algorithms, including four adaptive kNN models, i.e., PL-kNN [15], SMKNN [3], LMKNN [3], LV-kNN [9] and five graph-based kNN models i.e., the Centered kNNG [28], AKNNG [5], MAKNNG [5], mutual kNNG [21], and plain kNNG<sup>2</sup>. Additionally, to test the effectiveness of the proposed adaption criteria, we also include a version of DaNNG where we set aside the constraints during optimization, denoted as DaNNG(plain). Table 1 provides information on twelve

<sup>2</sup>Model abbreviation is consistent with how it’s described in original works, and all implementations of both SOTAs and DaNNG are publicly available.

included datasets obtained from UCI Machine Learning Lab, except for the Diabetes dataset [26] which was sourced from Kaggle.

To ensure objectivity prior to assessment, rigorous preprocessing has been applied to the data, and a uniform pre-configuration has been implemented for all algorithms. Detailed data sources and preprocessing methodologies are presented in *Appendices*.

### 6.2 Overall Performance

The performance matrix in Table 2 showcases the accuracy of different algorithms on each dataset. Across multiple datasets, DaNNG consistently demonstrates strong performance. Notably, on five datasets: BCC, Heart Disease, Glass, Diabetes, and Wine, DaNNG outperforms all other competing algorithms. Our model also exhibits the highest average accuracy among all twelve datasets. We also provide the marco F1-score to assess overall effectiveness of DaNNG in scenarios with multi-class and class imbalanced classifications. Table 3 shows that DaNNG also consistently outperforms competing SOTAs with respect to F1-score.

Significantly, while DaNNG(plain) demonstrates substantial robustness across multiple datasets, augmenting the optimization process with the proposed constraints further enhances our model’s performance. The improvements achieved by DaNNG, in terms of both accuracy and F1-score in comparison to DaNNG(plain), serve as validation for the effectiveness of the criteria introduced in Section 4.2.2.

## 7 DISCUSSION

In this section, we conduct a detailed examination of our model’s performance, with particular attention to its comparison with kNNG. Our model introduces distribution information into the graph construction of kNNG and, significantly, outperforms kNNG in 11 out of 12 datasets. This strong performance advantage sets the stage for an in-depth comparison that underscores the merits of our approach in enhancing classification outcomes.

### 7.1 Sensitivity of the Trade-Off Parameter

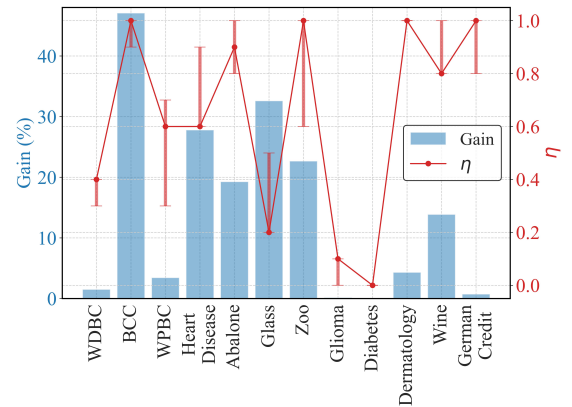


Figure 3: Performance gain of DaNNG concerning kNNG and the corresponding optimal trade-off  $\eta$  with error bar.

Dataset	PL-kNN	SMKNN	LMKNN	LV-kNN	AKNNG	MAKNNNG	Centered kNNNG	Mutual kNNNG	kNNNG	DaNNNG (plain)	DaNNNG
WDBC	0.9086	0.8999	0.8981	0.9174	0.9192	0.9210	0.9050	0.9192	0.9157	<b>0.9315</b>	0.9294
BCC	0.3652	0.2705	0.3515	0.3576	0.4485	0.4568	0.2720	0.4008	0.3750	0.3801	<b>0.5515</b>
WPBC	0.6989	0.7092	<b>0.7639</b>	0.7489	0.7334	0.7334	0.6987	0.7237	0.7337	0.7578	0.7589
Heart Disease	0.3242	0.2951	0.3302	0.3291	0.2555	0.2626	0.3516	0.3423	0.3143	0.3434	<b>0.4016</b>
Abalone	0.2217	0.2274	0.2200	0.2459	0.2049	0.1994	0.2298	0.2298	0.2286	<b>0.2906</b>	0.2726
Glass	0.5167	0.3758	0.2641	0.4251	0.5216	0.5262	0.4805	0.5301	0.4290	0.4290	<b>0.5688</b>
Zoo	0.9400	0.9100	0.7309	0.8500	0.9400	<b>0.9600</b>	0.7800	0.8200	0.7800	0.9400	0.9567
Glioma	0.8296	0.8022	0.8081	<b>0.8535</b>	0.8152	0.8032	0.8163	0.8188	0.8475	0.8475	0.8487
Diabetes	0.6420	0.6536	0.6510	0.6991	0.6692	0.6588	0.6561	0.6925	<b>0.7096</b>	<b>0.7096</b>	<b>0.7096</b>
Dermatology	0.8013	<b>0.8637</b>	0.7685	0.7736	0.7956	0.7983	0.7957	0.7872	0.7681	0.7953	0.8011
Wine	0.7261	0.6690	0.5490	0.7026	0.7363	0.7418	0.6278	0.6791	0.6912	0.7186	<b>0.7869</b>
German Credit	0.7030	0.6940	0.7000	0.6990	0.6940	0.6790	0.6400	0.7020	0.7080	<b>0.7200</b>	0.713
<b>Average</b>	<b>0.6398</b>	<b>0.6142</b>	<b>0.5863</b>	<b>0.6335</b>	<b>0.6445</b>	<b>0.6450</b>	<b>0.6045</b>	<b>0.6371</b>	<b>0.6251</b>	<b>0.6552</b>	<b>0.6916</b>

Table 2: Accuracy of 9 SOTAs and DaNNNG on 12 Datasets.

Dataset	PL-kNN	SMKNN	LMKNN	LV-kNN	AKNNG	MAKNNNG	Centered kNNNG	Mutual kNNNG	kNNNG	DaNNNG (plain)	DaNNNG
WDBC	0.8966	0.9001	0.9025	0.9036	0.8858	0.8859	0.8752	0.8722	0.8987	<b>0.9087</b>	0.8991
BCC	0.2637	0.2840	0.3285	0.3367	0.2014	0.2551	0.1848	0.2212	0.2628	0.2628	<b>0.3713</b>
WPBC	0.4539	0.4167	0.5343	0.5519	0.4555	0.4694	0.5480	0.4305	0.4534	0.4627	<b>0.5792</b>
Heart Disease	0.1927	0.2090	0.1690	0.1951	<b>0.2798</b>	0.2014	0.1844	0.1732	0.1785	0.2176	0.2622
Abalone	0.1493	0.1606	0.1320	0.1320	0.1240	0.0882	0.0544	0.0544	0.1526	0.1691	<b>0.1719</b>
Glass	0.2333	0.2931	0.2843	0.2790	0.2800	0.2767	0.1948	0.2033	0.2306	0.2482	<b>0.3355</b>
Zoo	0.6246	0.6714	0.8607	<b>0.9190</b>	0.6262	0.9057	0.8395	0.6468	0.7432	0.8588	0.9089
Glioma	0.4970	0.4833	0.4865	0.4773	0.4877	0.4914	0.4811	0.4829	0.4987	0.4987	<b>0.5071</b>
Diabetes	<b>0.6544</b>	0.6366	0.6163	0.6095	0.5971	0.5784	0.4240	0.4084	0.6381	0.6381	0.6381
Dermatology	0.7356	0.7618	0.7656	0.7703	0.7655	0.7652	<b>0.8381</b>	0.6562	0.6954	0.7424	0.7868
Wine	0.4056	0.3601	0.4170	0.4055	<b>0.4658</b>	0.4550	0.3807	0.3128	0.3792	0.3685	0.4414
German Credit	0.5781	0.5770	0.5839	0.5719	0.5950	0.4954	0.4337	0.4113	0.5633	<b>0.6050</b>	0.5950
<b>Average</b>	<b>0.4737</b>	<b>0.4795</b>	<b>0.5067</b>	<b>0.5126</b>	<b>0.4803</b>	<b>0.4890</b>	<b>0.4532</b>	<b>0.4061</b>	<b>0.4745</b>	<b>0.4984</b>	<b>0.5414</b>

Table 3: F1-Score of 9 SOTAs and DaNNNG on 12 Datasets.

The trade-off  $\eta$  is a crucial hyper-parameter of DaNNNG that balances the influence of the fitness kernel and traditional  $k$ . A higher  $\eta$  emphasizes the importance of the fitness kernel and hence the effectiveness of our proposal, while a lower  $\eta$  indicates possible unnecessary.

Figure 3 shows the percentage of accuracy gain of DaNNNG regarding kNNNG ( $gain = \frac{accuracy_{DaNNNG} - accuracy_{kNNNG}}{accuracy_{kNNNG}}$ ) under the optimal values of  $\eta$  in Section 6. From Figure 3, we observe a notable trend that as long as  $\eta$  is not close to zero, the accuracy gains consistently, with a maximum of 47.07% for BCC.

This finding underscores the significance of incorporating distribution approximation through the fitness kernel in our model. The higher  $\eta$  values indicate a stronger reliance on distribution-informed adaption, leading to improved classification performance.

## 7.2 Significant Improvement on Borderline Samples

As has been illustrated in Section 3.6, the mechanism behind the performance improvement of distribution-informed adaptive-k can be credited to the behavior of borderline samples. To evaluate the

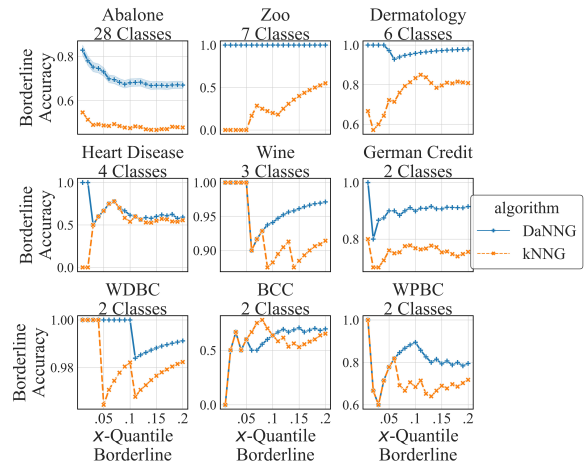


Figure 4: Borderline-sample accuracies of DaNNNG and kNNNG.

impact of our model on borderline samples, we analyze the performance gain of DaNNNG specifically on these samples.

We have computed the subsets of 1-Quantile Borderline to 20-Quantile Borderline for the aforementioned 9 datasets where  $\eta > 0.2$ . The accuracies on those borderline-sample subsets are shown in Figure 4. We observe significant improvements in borderline accuracies, especially in datasets involving a large number of classes. Improvements on binary classification are also consistently stable and notable, particularly with relatively larger datasets (i.e., WDBC and German Credit).

The considerable enhancement of borderline-sample performance of DaNNG provides insight for both the advancement of multi-class classifications and the dilemma of ambiguous decision boundaries.

## 8 CONCLUSION

In this article, we introduce DaNNG, a graph-based adaptive kNN model that integrates distribution approximation into the determination of  $k$  values. Through rigorous analysis, we establish that our approach generates a heterogeneous graph, significantly enhancing borderline accuracies and thereby improving overall model performance and robustness. Empirical evaluations demonstrate that DaNNG outperforms state-of-the-art adaptive kNN and graph-based kNN algorithms in various real-world scenarios. Notably, DaNNG not only achieves satisfied performance but also partially bypasses the necessity for normalization via the trade-off parameter  $\eta$ , enriching model flexibility. The model's adaptability and context-awareness position it as a potential solution for a wide range of real-world applications, particularly in class-imbalanced and multi-class scenarios.

## 9 APPENDICES

### REFERENCES

- [1] D. A. Adeniyi, Z. Wei, and Y. Yongquan. 2016. Automated Web Usage Data Mining and Recommendation System Using K-Nearest Neighbor (KNN) Classification Method. *Applied Computing and Informatics* 12, 1 (Jan. 2016), 90–108. <https://doi.org/10.1016/j.aci.2014.10.001>
- [2] Stefan Aeberhard and M. Forina. 1991. Wine. <https://archive.ics.uci.edu/dataset/109/wine>. Accessed: 2023-07-17.
- [3] Sarah M. Ayyad, Ahmed I. Saleh, and Labib M. Labib. 2019. Gene Expression Cancer Classification Using Modified K-Nearest Neighbors Technique. *Biosystems* 176 (Feb. 2019), 41–51. <https://doi.org/10.1016/j.biosystems.2018.12.009>
- [4] Antoine Boutet, Anne-Marie Kermarrec, Nupur Mittal, and Francois Taiani. 2016. Being Prepared in a Sparse World: The Case of KNN Graph Construction. In *2016 IEEE 32nd International Conference on Data Engineering (ICDE)*. IEEE, Helsinki, Finland, 241–252. <https://doi.org/10.1109/ICDE.2016.7498244>
- [5] Yongda Cai, Joshua Zhexue Huang, and Jianfei Yin. 2022. A New Method to Build the Adaptive K-Nearest Neighbors Similarity Graph Matrix for Spectral Clustering. *Neurocomputing* 493 (July 2022), 191–203. <https://doi.org/10.1016/j.neucom.2022.04.030>
- [6] Cheng-Hao Deng and Wan-Lei Zhao. 2018. Fast K-Means Based on k-NN Graph. In *2018 IEEE 34th International Conference on Data Engineering (ICDE)*. IEEE, Paris, 1220–1223. <https://doi.org/10.1109/ICDE.2018.00115>
- [7] Richard Forsyth. 1990. Zoo. <https://archive.ics.uci.edu/dataset/111/zoo>. Accessed: 2023-07-17.
- [8] Cong Fu and Deng Cai. 2016. EFANNA : An Extremely Fast Approximate Nearest Neighbor Search Algorithm Based on kNN Graph. [arXiv:1609.07228 \[cs\]](https://arxiv.org/abs/1609.07228)
- [9] N. Garcia-Pedrajas, J.A. Romero Del Castillo, and G. Cerruela-Garcia. 2017. A Proposal for Local  $k$  Values for  $k$ -Nearest Neighbor Rule. *IEEE Transactions on Neural Networks and Learning Systems* 28, 2 (2017), 470–475. <https://doi.org/10.1109/TNNLS.2015.2506821>
- [10] B. German. 1987. Glass Identification. <https://archive.ics.uci.edu/dataset/42/glass+identification>. Accessed: 2023-07-17.
- [11] Hans Hofmann. 1994. Statlog (German Credit Data). <https://archive.ics.uci.edu/dataset/144/statlog+german+credit+data>. Accessed: 2023-07-17.
- [12] Kunshan Huang, Shutao Li, Xudong Kang, and Leyuan Fang. 2016. Spectral-Spatial Hyperspectral Image Classification Based on KNN. *Sensing and Imaging* 17 (2016), 1–13.
- [13] Nilsel Ilter and H. Guvenir. 1998. Dermatology. <https://archive.ics.uci.edu/dataset/33/dermatology>. Accessed: 2023-07-17.
- [14] Andras Janosi, William Steinbrunn, Matthias Pfisterer, and Robert Detrano. 1988. Heart Disease. <https://archive.ics.uci.edu/dataset/45/heart+disease>. Accessed: 2023-07-17.
- [15] Danilo Samuel Jodas, Leandro Aparecido Passos, Ahsan Adeel, and Joao Paulo Papa. 2022. PL-k NN: A Parameterless Nearest Neighbors Classifier. In *2022 29th International Conference on Systems, Signals and Image Processing (IWSSIP)*. IEEE, Sofia, Bulgaria, 1–4. <https://doi.org/10.1109/IWSSIP55020.2022.9854445>
- [16] R. Kothari and V. Jain. 2002. Learning from Labeled and Unlabeled Data. In *Proceedings of the 2002 International Joint Conference on Neural Networks. IJCNN'02 (Cat. No.02CH37290)*. IEEE, Honolulu, HI, USA, 2803–2808. <https://doi.org/10.1109/IJCNN.2002.1007592>
- [17] Sankha Subhra Mullick, Shounak Datta, and Swagatam Das. 2018. Adaptive Learning-Based  $k$ -Nearest Neighbor Classifiers With Resilience to Class Imbalance. *IEEE Transactions on Neural Networks and Learning Systems* 29, 11 (Nov. 2018), 5713–5725. <https://doi.org/10.1109/TNNLS.2018.2812279>
- [18] Nils Murrugarra-Llerena and Alneu Andrade Lopes. 2011. An Adaptive Graph-Based  $K$ -nearest Neighbor. In *European Conference on Machine Learning and Principles and Practice of Knowledge Discovery in Databases*. 1–11.
- [19] Warwick Nash, Tracy Sellers, Simon Talbot, Andrew Cawthorn, and Wes Ford. 1995. Abalone. <https://archive.ics.uci.edu/dataset/1/abalone>. Accessed: 2023-07-17.
- [20] Hien Nguyen, Eric Cooper, and Katsuari Kamei. 2011. Borderline Over-Sampling for Imbalanced Data Classification. *International Journal of Knowledge Engineering and Soft Data Paradigms* 3 (April 2011), 4–21. <https://doi.org/10.1504/IJKESDP.2011.039875>
- [21] Kohei Ozaki, Masashi Shimbo, Mamoru Komachi, and Yuji Matsumoto. 2011. Using the Mutual  $K$ -Nearest Neighbor Graphs for Semi-Supervised Classification of Natural Language Data. In *Proceedings of the Fifteenth Conference on Computational Natural Language Learning (CoNLL '11)*. Association for Computational Linguistics, USA, 154–162.
- [22] Zhibin Pan, Yikun Wang, and Yiwei Pan. 2020. A New Locally Adaptive  $k$ -Nearest Neighbor Algorithm Based on Discrimination Class. *Knowledge-Based Systems* 204 (Sept. 2020), 106185. <https://doi.org/10.1016/j.knsys.2020.106185>
- [23] Miguel Patricio, Jos Pereira, Joana Crisostomo, Paulo Matafome, Raquel Seia, and Francisco Caramelo. 2018. Breast Cancer Coimbra. <https://archive.ics.uci.edu/dataset/451/breast+cancer+coimbra>. Accessed: 2023-07-17.
- [24] José A. Sáez, Julián Luengo, Jerzy Stefanowski, and Francisco Herrera. 2015. SMOTE-IPF: Addressing the Noisy and Borderline Examples Problem in Imbalanced Classification by a Re-Sampling Method with Filtering. *Information Sciences* 291 (Jan. 2015), 184–203. <https://doi.org/10.1016/j.ins.2014.08.051>
- [25] Jack W. Smith, J.E. Everhart, W.C. Dickson, W.C. Knowler, and R.S. Johannes. 1988. Pima Indians Diabetes Database. <https://www.kaggle.com/datasets/uciml/pima-indians-diabetes-database?resource=download>. Accessed: 2023-07-17.
- [26] Jack W. Smith, J.E. Everhart, W.C. Dickson, W.C. Knowler, and R.S. Johannes. 1988. Using the ADAP Learning Algorithm to Forecast the Onset of Diabetes Mellitus. *Proceedings of the Annual Symposium on Computer Application in Medical Care* 10 (Nov. 1988), 261–265.
- [27] Shiliang Sun and Rongqing Huang. 2010. An Adaptive  $K$ -Nearest Neighbor Algorithm. In *2010 Seventh International Conference on Fuzzy Systems and Knowledge Discovery*. IEEE, Yantai, China, 91–94. <https://doi.org/10.1109/FSKD.2010.5569740>
- [28] Ikumi Suzuki and Kazuo Hara. 2017. Centered  $k$ NN Graph for Semi-Supervised Learning. In *Proceedings of the 40th International ACM SIGIR Conference on Research and Development in Information Retrieval*. ACM, Shinjuku Tokyo Japan, 857–860. <https://doi.org/10.1145/3077136.3080662>
- [29] Erdal Tasci, Kevin Camphausen, Andra Valentina Krauze, and Ying Zhuge. 2022. Glioma Grading Clinical and Mutation Features Dataset. <https://archive.ics.uci.edu/dataset/759/glioma+grading+clinical+and+mutation+features+dataset>. Accessed: 2023-07-17.
- [30] Bruno Trstenjak, Sasa Mikac, and Dzenana Donko. 2014. KNN with TF-IDF Based Framework for Text Categorization. *Procedia Engineering* 69 (2014), 1356–1364. <https://doi.org/10.1016/j.proeng.2014.03.129>
- [31] William Wolberg. 1992. Breast Cancer Wisconsin (Original). <https://archive.ics.uci.edu/dataset/15/breast+cancer+wisconsin+original>. Accessed: 2023-07-17.
- [32] William Wolberg, Olvi Mangasarian, Nick Street, and W. Street. 1995. Breast Cancer Wisconsin (Diagnostic). <https://archive.ics.uci.edu/dataset/17/breast+cancer+wisconsin+diagnostic>. Accessed: 2023-07-17.
- [33] Yuanting Yan, Tianxiao Zhou, Zhong Zheng, Hao Ge, Yiwen Zhang, and Yanping Zhang. 2022. Robust Gravitation Based Adaptive  $k$ -NN Graph under Class-Imbalanced Scenarios. *Knowledge-Based Systems* 239 (March 2022), 108002. <https://doi.org/10.1016/j.knsys.2021.108002>
- [34] Shichao Zhang, Xuelong Li, Ming Zong, Xiaofeng Zhu, and Ruili Wang. 2018. Efficient  $k$ NN Classification With Different Numbers of Nearest Neighbors. *IEEE Transactions on Neural Networks and Learning Systems* 29, 5 (May 2018), 1774–1785. <https://doi.org/10.1109/TNNLS.2017.2673241>

## A DATA APPENDIX

The included datasets encompass a variety of domains and data complexities, ranging from medical diagnoses (e.g., Heart Disease, Diabetes, and Dermatology) to physical properties (e.g., Abalone, Glass, and Wine). The number of instances varies from small datasets like Zoo to larger datasets like Abalone. The model’s performance is evaluated on these datasets to assess its adaptability and generalization capability across different real-world scenarios. Detailed data resources are in Table 4.

Dataset	Resource
WDBC [32]	UCI
BCC [23]	UCI
WPBC [31]	UCI
Heart Disease [14]	UCI
Abalone [19]	UCI
Glass [10]	UCI
Zoo [7]	UCI
Glioma [29]	UCI
Diabetes [25]	Kaggle
Dermatology [13]	UCI
Wine [2]	UCI
German Credit [11]	UCI

**Table 4: Resources of included datasets.**

## B CODE APPENDIX

Our evaluations are conducted under Python3 with package requirement specified in Table 5. All 10 algorithms (including DaNNG) are implemented as a sklearn classifier with functions,  $fit(\cdot)$  and  $predict(\cdot)$ <sup>3</sup>.

Package	Version
networkx	2.8.8
numpy	1.21.2
pandas	1.3.3
scikit-learn	1.1.3
scipy	1.7.1
prda	1.1.0

**Table 5: Python package requirements of evaluations.**

Before conducting the experiments, datasets are preprocessed to ensure uniformity. The following preprocessing steps are applied:

- Samples without the prediction target are dropped from datasets.
- Samples with missing values in features are filled with the mean value of the corresponding feature.
- Numerical features are normalized before fitting, and categorical features are preprocessed with one-hot encoder.

Models are pre-configured as follows:

- Models which require a pre-defined  $k$  are set to 10, and those that require a pre-defined  $k$  boundary ( $k_{min}$  and  $k_{max}$ ) are set to 5 and 15, respectively.
- Graph-based algorithms, including our DaNNG, use the majority vote strategy to make predictions, meaning that the majority class of neighbors of the closest node for each test sample is applied as the prediction.
- In DaNNG, the trade-off parameter  $\eta$  is set to range (0, 1) with an interval of 0.1 in order to assess the degree of importance of  $F$ , and the KDE bandwidth  $h$  is set to 0.5.
- The performance is evaluated by measuring prediction accuracy under 10-fold cross-validation.

<sup>3</sup>All implementations are available in: <https://github.com/4alexmin/knnsotas>